11. D. S. Citrin, *Phys. Rev. B* **47**, 3832 (1993).
12. U. Bockelmann, *ibid.* **48**, 17637 (1993).
13. H. Benisty, *ibid.* **51**, 13281 (1995).
14. D. Gammon, E. S. Snow, B. V. Shanabrook, D. S. Katzer, D. Park, *Phys. Rev. Lett.* **76**, 3005 (1996).
15. H. W. van Kesteren, E. C. Cosman, W. A. J. A. van der Poel, C. T. Foxon, *Phys. Rev. B* **41**, 5283 (1990).
16. E. Blackwood, M. J. Snelling, R. T. Harley, S. R. Andrews, C. T. B. Foxon, *ibid.* **50**, 14246 (1994).
17. To obtain this result, we used the measured spectrometer response function and assumed that the excitonic ground-state line shape is Lorentzian, as observed for the excited states (left inset, Fig. 2).
18. The homogeneous linewidth is determined by the total dephasing rate which in general is given by the exciton lifetime term τ^{-1} discussed in the text plus a pure dephasing term [see, for example, M. D. Webb, S. T. Cundiff, D. G. Steel, *Phys. Rev. B* **43**, 12658 (1991)]. For resonant excitation of a single Qdot at low temperature and power density, the pure dephasing rate should be small, and we ignore it in our discussion. We take $\tau^{-1} = \Gamma$ (FWHM)/$\hbar$, where $\hbar$ is Planck's constant divided by 2π.
19. A. Vinattieri *et al.*, *Phys. Rev. B* **50**, 10868 (1994).
20. In this sense our localized exciton system is qualitatively different from that examined in the earlier linewidth studies (*1–5*). This difference arises from the use of growth interrupts at the interfaces in our samples, which completely changes the spectral and spatial distribution of the localized states [see, for example, D. Gammon *et al.*, *Appl. Phys. Lett.* **57**, 2710 (1990)].
21. L. C. Andreani, F. Tassone, F. Bassani, *Solid State Commun.* **77**, 641 (1991); L. C. Andreani in *Confined Electrons and Photons*, E. Burstein and C. Weisbuch, Eds. (Plenum, New York, 1995), p. 57.
22. B. Deveaud *et al.*, *Phys. Rev. Lett.* **67**, 2355 (1991).
23. J. Kuhl, A. Honold, L. Schultheis, C. W. Tu, *Festkoerperprobleme* **29**, 157 (1989).
24. Published values of γ for quantum wells vary from 2.5 μeVK^{-1} for a 12-nm quantum well, as shown in Fig. 3, to 9 μeVK^{-1} for a 28-nm quantum well (*23*).
25. V. Srinivas, Y. J. Chen, C. E. C. Wood, *Phys. Rev. B* **46**, 10193 (1992); D. Gammon, S. Rudin, T. L. Reinecke, D. S. Katzer, C. S. Kyona, *ibid.* **51**, 16785 (1995).

26. This research was funded in part by the office of Naval Research.

4 March 1996; accepted 15 May 1996

Two Calorimetrically Distinct States of Liquid Water Below 150 Kelvin

G. P. Johari,* Andreas Hallbrucker, Erwin Mayer

Vapor-deposited amorphous solid and hyperquenched glassy water were found to irreversibly transform, on compression at 77 kelvin, to a high-density amorphous solid. On heating at atmospheric pressure, this solid became viscous water (water B), with a reversible glass-liquid transition onset at 129 ± 2 kelvin. A different form of viscous water (water A) was formed by heating the uncompressed vapor-deposited amorphous solid and hyperquenched liquid water. On thermal cycling up to 148 kelvin, water B remained kinetically and thermodynamically distinct from water A. The occurrence of these two states, which do not interconvert, helps explain both the configurational relaxation of water and stress-induced amorphization.

Amorphous solid water can be prepared by vapor deposition on a metal substrate kept at 100 K or below (*1*). In 1980, it was first shown that liquid water, when cooled at rates of $\approx 10^6$ to $\approx 10^7$ K s^{-1}, also produced an amorphous solid known as hyperquenched glassy water (*2*). Four years later, it was observed that uniaxial compression of hexagonal ice to 10 kbar at 77 K produced a new amorphous solid (*3*) called high-density amorph (HDA). Its density of 1.31 g cm^{-3} at 77 K and 10 kbar decreases to 1.17 g cm^{-3} on decompression to 1 bar, and its x-ray and neutron diffraction patterns are quite distinct from those of the amorphous forms obtained from vapor deposition or by hyperquenching water, all at 1 bar (*3–6*). Cubic ice is also found to collapse in a similar manner to HDA (*7, 8*) but not ice clathrate (*9*). On heating to 125 K at 1 bar, HDA (1.17 g cm^{-3}) transforms irreversibly and exothermally to a low-density amorph (LDA). This in turn undergoes a glass-to-liquid transition with an onset temperature of 129 ± 2 K (referred to as its T_g) on heating at 30 K min^{-1} (*8, 10*) or of 124 K on heating at 0.17 K min^{-1} (*11*). Upon further heating to far above its T_g, the now metastable state of viscous liquid water crystallizes to cubic ice extremely rapidly at $\approx$150 K.

In our continuing experimental studies of the thermodynamics of the solid forms of amorphous water, we have discovered that vapor-deposited amorphous solid water and hyperquenched glassy water, whose T_g values are both 136 ± 1 K for heating at 30 K min^{-1} (*12, 13*), collapse also under a uniaxial pressure to produce a high-density amorphous solid at 77 K. On heating at 1 bar, this solid transforms exothermally and irreversibly to a low-density amorphous solid that, on further heating, undergoes a glass-to-liquid transition at 129 ± 2 K for heating at 30 K min^{-1}. This T_g is the same as that of LDA obtained by uniaxial compression of hexagonal and cubic ices at 77 K (*8, 10*).

Thus, we report here two effects: first, under a uniaxial pressure at 77 K, the amorphous solids—namely, the vapor-deposited amorphous solid water (ASW), the hyperquenched glassy water (HGW), and the crystalline solids (hexagonal and cubic ices)—all collapse to produce HDA. On heating to 125 K at 1 bar, this amorph transforms irreversibly to LDA with T_g = 129 K. Second, this LDA is calorimetrically distinct from ASW and HGW (*12, 13*), although the densities of the three are similar.

Further experiments show that there are two distinct forms of viscous water: water A, which is obtained by heating uncompressed ASW and HGW to above T_g = 136 K and up to 148 K, and water B, which is obtained by heating, at 1 bar, the product of uniaxially compressed ASW, HGW, and hexagonal and cubic ices to 148 K, a temperature above the T_g (129 K) of the amorphous solids. This has implications for our understanding of the water's state in the extraterrestrial bodies where high pressures exist (*14*); here, we consider its implications only for our understanding of irreversible phase transformations under pressure and of configurational relaxations in liquid water.

Vapor-deposited amorphous water (ASW) was prepared by admitting water vapors from a water reservoir held at 298 K through a fine metering valve and a tube of 13 mm inner diameter into a high vacuum system, where the vapors condensed on a demountable Cu substrate (50 mm diameter) precooled to 77 K (*12, 15*). In control experiments of our ASW deposits by x-ray diffraction, no sharp peaks (indicating crystalline ice) were observed (*12*). Because our x-ray technique is sensitive to a crystallinity of >2%, we infer that our ASW was at least 98% amorphous. It was then heated in a vacuum to $\approx$115 K for reduction of its surface area and closure of micropores, before its exposure to N_2. ASW treated this way is called "sintered." A similar treatment has been used in the glass-to-liquid transition of ASW (*12*).

Glassy water (HGW) was prepared by hyperquenching—that is, by acceleration of droplets of water ($\approx$3 μm diameter) from an aerosol by supersonic flow and then by their deposition on a Cu plate held inside a high-vacuum cryostat at 77 K (*13, 16*). One hour of deposition produced a 2- to 3-mm-thick opaque layer of glassy solid water with a porcelainlike appearance and texture. According to x-ray diffractograms, it contained

G. P. Johari, Department of Materials Science and Engineering, McMaster University, Hamilton, Ontario L8S 4L7, Canada.
A. Hallbrucker and E. Mayer, Institut für Allgemeine, Anorganische und Theoretische Chemie, Universität Innsbruck, A-6020 Innsbruck, Austria.

---

*To whom correspondence should be addressed.

at most 5% crystalline, mainly cubic, ice (*13, 16*). All transfers of the sample from one container to the other were made when it was immersed in liquid N_2.

A piston-cylinder apparatus with an 8-mm-diameter piston was used for the compression of sintered ASW and of HGW by means of a hydraulic press. The displacement of the piston was measured by a dial gauge as a function of pressure during both the compression and decompression of the solids at 77 K. The displacement-pressure curves for the sintered ASW and for the HGW samples were similar to those observed previously (*3, 7, 10, 12, 17*). At 77 K, sintered ASW and HGW began to transform into HDA at 2 kbar but required up to 6 kbar for complete transformation (*18*). For comparison, at the same temperature LDA and hexagonal ice transform into HDA under pressures of 6 ± 0.5 kbar (*17*) and 10 ± 1 kbar (*3*), respectively. This pressure drops to 2 kbar for the transformation of LDA into HDA at 135 K (*19*). Samples were recovered from the piston-cylinder apparatus at 77 K. The rate of pressure release at 77 K had no influence on the T_g value upon subsequent thermal treatment.

We first studied samples that had not been compressed. Between 15 and 26 mg of the samples was placed in a stainless steel capsule to obtain differential scanning calorimetry (DSC) scans at 1 bar, with the use of a Perkin-Elmer DSC model IV with a computer-based data acquisition system (*8, 10, 12, 13*). The samples were first annealed for 90 min at 130 K. DSC scans were then obtained for heating at 30 K min^{-1} from 115 to 165 K (Fig. 1, curves a and b for ASW and HGW, respectively). These annealing conditions have previously given maximal endothermic step height (*12, 13*). Other annealing temperatures or times affected only the height of the endothermic step but not its T_g value. Both scans show, as in earlier studies (*12, 13*), a glass-to-liquid transition with a T_g of 136 ± 1 K and an onset of crystallization at ≈149 K. The DSC scans of samples heated close to 150 K and then cooled to 103 K showed, during reheating, the same T_g of 136 ± 1 K. This means that the state of the metastable liquid above 136 K is continuous with that of the amorphous solid and that the glass-to-liquid transition is reversible. The increase in heat capacity in the glass-to-liquid transition region (ΔC_p) of 1.9 J K^{-1} mol^{-1} for ASW and of 1.6 J K^{-1} mol^{-1} for HGW, the width of the endotherm of 14 K and 12 K, respectively, and their crystallization exotherms are identical with those observed before (*12, 13*).

The DSC scan of HDA obtained by compression of ASW (Fig. 1, curve c) showed an exothermic feature centered at ≈132 K when HDA was transformed into LDA; the same feature was observed for HDA obtained by compression of HGW. This is identical with the behavior of HDA formed on compression of hexagonal and cubic ices (*3, 7, 8, 10*). When the HDA or LDA samples were annealed for 90 min at 127 K, cooled at 30 K min^{-1} to 103 K, and thereafter reheated to 148 K, their DSC scans (curve d) showed a glass transition endotherm with a T_g of 129 ± 2 K and ΔC_p of 1.8 ± 0.2 J K^{-1} mol^{-1}, irrespective of whether the sample was originally prepared from ASW or HGW. Reheating for a second time (curve e, recorded after curve d) demonstrates the reversibility of the glass-to-liquid transition. The same glass transition features had been observed in our earlier studies of pressure-amorphized hexagonal ice and cubic ice (*8, 10*) and are included for comparison in Fig. 1 (curves g and h). Keeping a compressed ASW sample for up to 60 s at 148 K, cooling to 103 K, and reheating at 30 K min^{-1} still showed the T_g at 129 K, even if the height of the endothermic step was reduced by up to 60% by crystallization. Evidently, the glass transition of metastable equilibrium liquid water is (at 148 K) thermally reversible and its state over the range of 103 K to 148 K is thermodynamically continuous with that of LDA.

These experiments demonstrate that even at 148 K, the metastable equilibrium water with a T_g of 129 K, water B, cannot be transformed to a (structural) state that is continuous with ASW and HGW, a state with a T_g of 136 K (water A). Several attempts were made to convert ASW and HGW (T_g = 136 K) into LDA (T_g = 129 K) by heating ASW and HGW samples close to 150 K at a rate of 10 or 30 K min^{-1}. We observed only a decrease in the height of the endothermic step caused by partial crystallization of the sample, but no change in the T_g value. So, even at temperatures close to 150 K, the structural state of viscous water obtained from LDA remains separated from the state obtained by heating ASW and HGW, or the two states of liquid are not interconvertible. The sketch in Fig. 2 describes these and the previous observations of pressure-amorphizing cubic (*7, 8*) and hexagonal (*3, 7, 10, 11*) ices. Water B, which forms on heating LDA above its T_g, can be obtained by compression of the crystalline as well as of the noncrystalline solid forms. The difference of 7 K between the T_g values of HGW and ASW at 136 K and that of LDA at 129 K is a reflection of a basic difference between their H-bonded structures.

For the LDA forms of uniaxially compressed HGW or ASW, the enthalpy of crystallization to cubic ice is about 10% lower than those of the uncompressed solids (*12, 13*). Assuming that the cubic ice phases formed in both cases have the same enthalpy, this would imply a smaller enthalpy value for the LDA forms than for ASW and HGW. However, a smaller value would also be obtained if a small amount of the sample had crystallized during the pres-

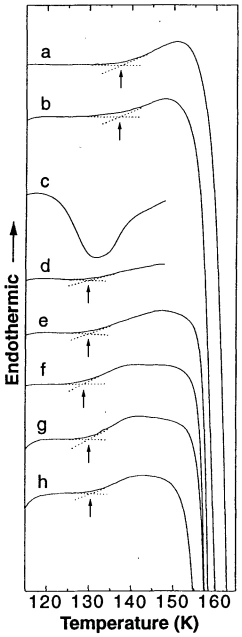

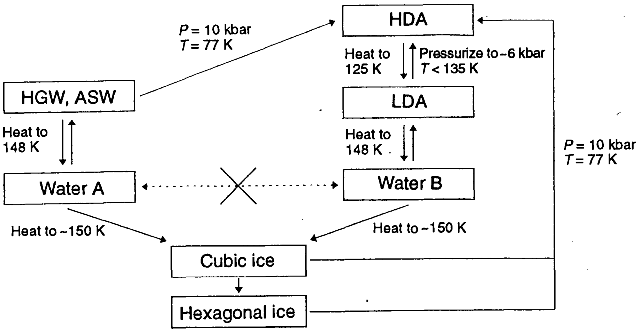

Fig. 1 (left). The glass-to-liquid transition and crystallization in amorphous water samples as seen in DSC scans recorded on heating at 30 K min^{-1}. Curves a and b are the scans of sintered ASW and of HGW; curve c shows the heat released upon first heating to 148 K during conversion of HDA, obtained by uniaxial compression of sintered ASW, to LDA; curves d and e show the endothermic step on second heating to 148 K (curve d) and on third heating (curve e) for the same ASW sample used for curve c; curve f is LDA from uniaxially compressed HGW; curves g and h show LDA from the pressure-collapsed state of hexagonal and cubic ice (*8, 12*). The curves are drawn on the same scale but are shifted vertically for clarity. The temperatures are not corrected for thermal lag of the instrument (which is −1.5° for heating at 30 K min^{-1}). The T_g values depend to some extent on the way the tangents are drawn for determining their intersection. This is taken into account by our error estimate. Arrows indicate the direction in which transitions occur. **Fig. 2 (right).** A schematic representation for the formation of the two distinct states of metastable equilibrium liquid water, water A and water B, which are not interconvertible upon heating up to 148 K.

surizing procedure. At present, we cannot differentiate between these two cases.

On heating to 148 K at 1 bar, the solid HGW, ASW, and LDA became highly viscous liquids with a structural relaxation time of less than 1 s, as calculated previously (*13*). On cooling to below 136 K, water A that was obtained from heating solid HGW and ASW transformed back to the same solids, and on cooling to below 129 K, water B that was obtained from heating solid LDA transformed back to LDA. There is no path by which HGW or ASW can be connected to LDA at a constant pressure or by which water A could be connected to water B. That is, water A and water B are thermodynamically discontinuous states at 1 bar and are calorimetrically distinct from each other. Both irreversibly transform to cubic ice upon heating above 150 K but do not transform from one to the other.

We conclude that the structure of metastable liquid obtained by heating brittle solid HGW and ASW differs from that obtained by heating brittle solid LDA. This means that in water, where molecules form a variety of H-bonded structures of different energies and volume, configurational or structural relaxation within the same average energy and volume of certain states can be preferable to transformation to a state of lower energy and different volume (a similar situation is found in certain chemical reactions in which low viscosity or fast configurational relaxation of the reactants does not facilitate a reaction, whereas increased thermal energy does). In this sense, the metastable equilibrium structures of H bonds in the two states of water, water A and water B, below 150 K remain separated by potential energy barriers too high to be overcome by thermal energy.

A single amorphous solid, either ASW or HGW, produces both water A and water B (Fig. 2). Water A is formed by heating the amorphous solids; water B is formed by first converting ASW or HGW (or hexagonal or cubic ices) to HDA by uniaxial compression, heating HDA to transform it to LDA, and then heating LDA. Water A and water B are not interconvertible reversibly by thermal cycling alone, although they are interconvertible by indirect paths that involve irreversible phase transformations and uniaxial compression. These results help clarify several aspects of the stress-induced phase transitions from one amorphous solid to another and have implications for the results obtained from a wide variety of computer simulations on the structure of metastable water (*20–30*).

It is important to note here that Fisher and Devlin (*31*) suggested from their infrared study of vapor-deposited amorphous water containing 0.1 mol% 2-naphthol that there is no translational diffusion in the amorphous solid up to 125 K. This temperature is much less than the T_g of 136 K for pure ASW, and therefore translational diffusion is expected to take a much longer time at 125 K than at 136 K. Also, the 0.1 mol% 2-naphthol in their samples makes their studies less relevant to our studies of pure water. For these reasons, an intercomparison between the two studies is irrelevant.

Recent studies have shown that ASW and HGW can be thermodynamically continuous with normal supercooled water (*32*, *33*). Water A, which is formed on heating ASW and HGW, should therefore also be thermodynamically continuous with supercooled water, even though it forms upon the structural relaxation and heating of HGW (*13*) or of sintered ASW rather than during the course of hyperquenching or vapor deposition (*12*). This is in contrast to the conjecture that the liquid water formed upon heating ASW and HGW is thermodynamically discontinuous with supercooled water and that the former should therefore be regarded as a new phase, water II (*34*).

Because several groups have attempted to verify this experimentally (*32*, *33*, *35*, *36*) and by computer simulation (*37*) it bears examination in relation to our results. First, the inference of thermodynamic discontinuity between water at 150 K and water at 273 K, which led to conjectures of the existence of water II at 150 K and water I at 273 K (*34*), has been refuted by a direct analysis of new, more accurate data that demonstrated instead a thermodynamic continuity (*32*). Second, the conjectures of the thermodynamic and viscosity behaviors of water II, which were based on a comparison of the DSC scan of ASW with that of 8.33 mol% LiCl aqueous solution (*36*), have found support neither from a reinvestigation nor from fundamental reasoning (*35*). Third, vapor pressure measurements of ASW (*33*) have shown that the properties of water II can be thermodynamically continuous with those of water I, thus eliminating the need to consider them separate phases. We must conclude that the conjectures for water II were based on inadequate information and that water A, water II (both formed by heating ASW and HGW to 148 K), and water I (normal water at 273 K, or supercooled) are the same liquid. Water B is a new phase whose incorporation in a phase diagram requires further experiments.

REFERENCES AND NOTES

1. E. F. Burton and W. F. Oliver, *Proc. R. Soc. London Ser. A* **153**, 166 (1935).
2. P. Brüggeller and E. Mayer, *Nature* **288**, 569 (1980).
3. O. Mishima, L. D. Calvert, E. Whalley, *ibid.* **310**, 393 (1984).
4. L. Bosio, G. P. Johari, J. Teixeira, *Phys. Rev. Lett.* **56**, 460 (1986).
5. M. A. Floriano, E. Whalley, E. C. Svensson, V. F. Sears, *ibid.* **57**, 3062 (1986).
6. M.-C. Bellisent-Funel, J. Teixeira, L. Bosio, *J. Chem. Phys.* **87**, 2231 (1987).
7. M. A. Floriano, Y. P. Handa, D. D. Klug, E. Whalley, *ibid.* **91**, 7187 (1989).
8. G. P. Johari, A. Hallbrucker, E. Mayer, *J. Phys. Chem.* **94**, 1212 (1990).
9. G. P. Johari and S. J. Jones, *Philos. Mag.* **B54**, 311 (1986).
10. A. Hallbrucker, E. Mayer, G. P. Johari, *J. Phys. Chem.* **93**, 7751 (1989).
11. Y. P. Handa and D. D. Klug, *ibid.* **92**, 3323 (1988).
12. A. Hallbrucker, E. Mayer, G. P. Johari, *ibid.* **93**, 4986 (1989).
13. G. P. Johari, A. Hallbrucker, E. Mayer, *Nature* **330**, 552 (1987); *J. Chem. Phys.* **92**, 6742 (1990).
14. E. Whalley, in *Ices in the Solar System*, NATO ASI Series, vol. 156, J. Klinger, D. Benest, A. Dollfus, R. Smoluchowski, Eds. (Reidel, Dordrecht, 1984), pp. 9–37.
15. A. Hallbrucker and E. Mayer, *J. Chem. Soc. Faraday Trans.* **86**, 3785 (1990).
16. E. Mayer, *J. Appl. Phys.* **58**, 663 (1985); *J. Phys. Chem.* **89**, 3474 (1985); *ibid.* **90**, 4455 (1986).
17. O. Mishima, L. D. Calvert, E. Whalley, *Nature* **314**, 76 (1985).
18. The range of pressure needed for complete transformation was a reflection of the difficulty in plastic flow required to convert the uniaxial stress to a hydrostatic stress in a relatively narrow pressure vessel.
19. O. Mishima, *J. Chem. Phys.* **100**, 5910 (1994); but see also G. P. Johari, *ibid.* **102**, 6224 (1995), where further analysis was done.
20. F. H Stillinger, *Science* **209**, 451 (1980).
21. R. J. Speedy, *J. Phys. Chem.* **88**, 3364 (1984); _____ and M. Mezei, *ibid.* **89**, 171 (1985); R. J. Speedy, J. D. Madura, W. L. Jorgensen, *ibid.* **91**, 909 (1987).
22. J. S. Tse and M. L. Klein, *Phys. Rev. Lett.* **58**, 1672 (1987); *J. Phys. Chem.* **92**, 315 (1988); *J. Chem. Phys.* **92**, 3992 (1990); J. S. Tse, *ibid.* **96**, 5482 (1992).
23. R. L. Blumberg, , H. E. Stanley, A. Geiger, P. Mausbach, *J. Chem. Phys.* **80**, 5230 (1984); F. Sciortino, A. Geiger, H. E. Stanley, *Nature* **354**, 218 (1991); *J. Chem. Phys.* **96**, 3857 (1992); A. Geiger, N. N. Medvedev, Yu. I. Naberukhin, *Zh. Strukt. Khim.* **33**, 79 (1992).
24. P. A. Giguere, *J. Chem. Phys.* **87**, 4835 (1987).
25. P. H. Poole, F. Sciortino, U. Essmann, H. E. Stanley, *Nature* **360**, 324 (1992); *Phys. Rev. E* **48**, 3799 (1993); *ibid.*, p. 4605; H. E. Stanley *et al.*, *Physica A* **205**, 122 (1994); P. H. Poole, F. Sciortino, T. Grande, H. E. Stanley, C. A. Angell, *Phys. Rev. Lett.* **73**, 1632 (1994).
26. C. F. Wong, C. Zheng, J. A. McCammon, *Chem. Phys. Lett.* **154**, 151 (1989).
27. A. R. Henn and W. Kauzmann, *J. Phys. Chem.* **93**, 3770 (1989).
28. Q. Zhang and V. Buch, *J. Chem. Phys.* **92**, 5004 (1990); V. Buch, *ibid.* **96**, 3814 (1992).
29. G. E. Walrafen and Y. C. Chu, *J. Phys. Chem.* **99**, 10635 (1995).
30. G. Corongiu and E. Clementi, *J. Chem. Phys.* **97**, 2030 (1992); *ibid.* **98**, 2241 (1993).
31. M. Fisher and J. P. Devlin, *J. Phys. Chem.* **99**, 11584 (1995).
32. G. P. Johari, G. Fleissner, A. Hallbrucker, E. Mayer, *ibid.* **98**, 4719 (1994).
33. R. J. Speedy, P. G. Benedetti, C. Huang, R. C. Smith, B. D. Kay, in *Physical Chemistry of Aqueous Systems: Meeting the Needs of Industry*, proceedings of the 12th International Conference on the Properties of Water and Steam, H. J. White Jr., J. V. Sengers, D. B. Neumann, J. C. Bellows, Eds. (Begell House, New York, 1995), pp. 347–354.
34. R. J. Speedy, *J. Phys. Chem.* **96**, 2322 (1992).
35. E. Mayer, A. Hallbrucker, G. Sartor, G. P. Johari, *ibid.* **99**, 5161 (1995).
36. Ç. A. Angell, *ibid.* **97**, 6339 (1993).
37. H. Tanaka, *Nature* **380**, 328 (1996).
38. We are grateful for financial support by the Forschungsförderungsfonds of Austria (project P10404-PHY).

29 January 1996; accepted 13 May 1996